

INFLUENCE OF DIFFERENT STIFFENING TYPES OF THE AIRCRAFT BODY STRUCTURE ON THE NOISE EXPOSURE IN THE CABIN

Otto von Estorff, Thilo König
 Institute of Modelling and Computation
 Hamburg University of Technology

Keywords: *acoustics, calculation, stringer, BEM, transmission loss*

Abstract

The current paper deals with the influence of stiffeners on the sound transmission through aircraft structures. Several studies have shown that the vibrations of the stiffeners form a sound transmission path in a way that the movements of the stringers excite the “aircraft skin fields“, which leads to additional “noise sources”. Besides the investigation of this effect, the objective of the present contribution is the investigation of different modeling variants, the radiation of sound energy of vibrating stringers, and the influence of the stiffening on the skin field with respect to sound transmission. Within the investigations, a coupled Boundary Element/Finite Element Method has been used.

1 Introduction

When developing modern aircrafts, sound simulations are already carried out in the design phase, in order to be able to evaluate the noise exposure of the cabin interior before a prototype exists. These include the simulation of the sound transmission paths through the cabin wall as well as the sound radiation of single components. In particular, it is not only objected to determine the noise level perceived by the passenger, but also to optimize the acoustical behaviour of single components. Of course, the structural vibrations and the acoustics are closely related.

In the past, researchers spent quite some time in the computational investigation of the sound transmission through simple plane struc-

tures, see e.g. [1-4], but also curved and stiffened fuselage structures have been investigated [5-7]. When using numerical approaches, such as the Finite Element Method, different element types, namely solid, shell, and beam elements in combination with isotropic as well as layered materials are available and have been investigated, for instance, in [8-10].

Common aircraft structures consist of complicated geometries including complex stiffeners and skin fields where different numerical approaches and models can be applied to simulate their dynamic behavior. The effects of different modelling variants on the numerical results as well as their vibroacoustic effects have not been treated comprehensively yet.

The objective of this contribution is to evaluate the acoustic influence of important components of a fuselage structure. In particular, the influence of the stiffeners (of the body structure) with respect to their discretization, their structural vibration, and their sound radiation will be investigated and discussed. Furthermore the acoustical effects of panels with different stiffened regions are considered.

The first section deals with the numerical methods employed for the simulations. The governing equations are shown for the structural Finite Element Method (FEM) as well as for the Boundary Element Method (BEM) used for the acoustical part. Further on, the coupling of the FEM and the BEM is described. In the second section, the different modelling possibilities of stiffeners as well as the resulting computational effects on the structural behaviour are consid-

ered. Afterwards the influences of the stringers on the acoustical behaviour of structures will be discussed. The last section deals with the effects of local stiffening regions of a panel.

2 Calculation principles and governing equations

For the computation of the structural behaviour of the investigated systems the Finite Element Method is applied, while the indirect Boundary Element Method is employed to account for the acoustical effects. The FEM and the BEM are used simultaneously, leading to a coupled approach. All investigations will be performed in the frequency domain.

In the following, the two calculation methods are described briefly. A detailed derivation for the approaches can be found, e.g., in [9-13].

2.1 Structural calculation using FEM

The FEM is used to determine the mode shapes and eigenfrequencies of the vibrating structure. Both the shapes and the frequencies are essential inputs for the acoustical calculation.

Using the concept of virtual displacements, the equation of motion describing the dynamic behavior of the structure at a given frequency ω can be derived, such that

$$([K] + i\omega[D] - \omega^2[M]) \cdot \{U\} = \{F\} \quad (1)$$

The matrix $[K]$ is the stiffness matrix and $\{F\}$ is the vector of the frequency dependent excitation forces, $[D]$ and $[M]$ are the damping and mass matrix, respectively. The vector $\{U\}$ contains the unknown displacements in physical coordinates. In the case that the eigenvectors $\{\phi\}$ of the structure are known, its response can be calculated by a linear superposition of these eigenvectors:

$$\{U\} = \sum_{i=1}^n a_i \{\phi_i\} = [\Phi] \{a\}, \quad (2)$$

where $\{a\}$ denotes the vector of the “n” modal participation factors and $[\Phi]$ is the matrix of the respective eigenvectors. The unknown participation factors are obtained from:

$$\begin{aligned} &([\Phi]^T \cdot ([K] + i\omega[D] - \omega^2[M]) \cdot [\Phi]) \cdot \\ &\dots \cdot \{a\} = [\Phi]^T \{F_S\} \end{aligned} \quad (3)$$

2.2 Acoustical calculation using BEM

For the acoustical part of the coupled vibro-acoustic model the BEM is employed. The approach is based on the solution of the Helmholtz equation

$$\nabla^2 p + k^2 p = 0 \quad (4)$$

where p is the sound pressure of the fluid, while $k = \omega/c$ is the wave number depending on the sound velocity c . The system of equations resulting from the indirect BE formulation can be written as [11]:

$$\begin{bmatrix} [B] & [C^T] \\ [C] & [D] \end{bmatrix} \begin{Bmatrix} \{\sigma\} \\ \{\mu\} \end{Bmatrix} = \begin{Bmatrix} \{f\} \\ \{g\} \end{Bmatrix}. \quad (5)$$

The unknown parameters $\{\sigma\}$ and $\{\mu\}$ are the single and double layer potentials, respectively, $\{f\}$ and $\{g\}$ are vectors containing the frequency dependent excitations of the system. From the potentials σ and μ at the surface of the sound radiating structure, the sound pressure at an arbitrary point p can then be obtained by employing

$$p_p = \{a\}^T \{\sigma\} + \{b\}^T \{\mu\}, \quad (6)$$

where the vectors $\{a^T\}$ and $\{b^T\}$ are influence coefficients which can be determined as described in [11].

2.3 Coupled FEM/BEM system

A combination of the Equations (1) and (6) leads to the system of equations

$$\begin{bmatrix} [\hat{K}] - \omega^2[M] & [\hat{C}^T] \\ [\hat{C}] & \frac{[H(\omega)]}{\rho\omega^2} \end{bmatrix} \begin{Bmatrix} \{a\} \\ \{\mu\} \end{Bmatrix} = \begin{Bmatrix} \frac{\hat{F}}{\rho\omega^2} \\ \frac{F_A}{\rho\omega^2} \end{Bmatrix} \quad (7)$$

which represents the coupled behavior of the structure and the surrounding air. $[H(\omega)]$ is the BEM influence matrix resulting from Equation (6) and $[C]$ the geometrical coupling matrix. The vectors $\{F\}$ and $\{F_A\}$ contain the excitation, while $\{a\}$ denotes the structural influence vectors. The “hat” symbol is used to mark the quantities expressed in the modal domain.

2.4 TL and the effect of coincidence

In order to evaluate the acoustical transmission of sound energy through the walls under investigation, the transmission loss [TL] is used. It is defined as the ratio of the excitation energy and the radiation energy of the structure. The mass law for a diffuse acoustic sound field, as applied later, is given by [14-15]:

$$R = 10 \log \left(1 + \left(\frac{m\omega}{2\rho c} \right)^2 \right) - 3 \quad [dB] \quad (7)$$

where m is the specific mass of the structure and ρc is the impedance of the adjacent fluid. The diffuse field approach, as used here, predicts a reduction of the TL by 3 dB, as shown in equation 8.

A typical curve of the TL is given in Fig. 1. The total frequency range is divided in three regions. The *first region* in the lower frequency band includes the “stiffness controlled” TL where no bending movements of the wall exist. By increasing the frequency, the resonances become evident, where the effects of the eigenmodes of the structure are dominant. The *second region* describes the mass law. In this area only the mass of the structure influences the curve. The TL increase by 6 dB per octave. The *third region* is characterised by the coincidence effect. The frequency f_c shown in the Fig. 1 denotes the coincidence frequency. At this frequency the wave length of the bending wave of the structure is equal to the wave length of the fluid. Considering the angle between the acoustical wave and the structure, the frequency dependence of the coincidence effect can be observed.

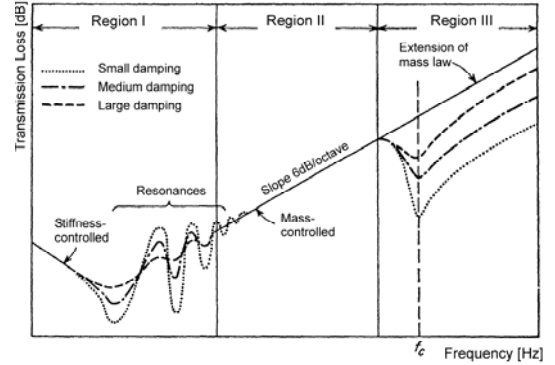


Fig. 1. Typical Transmission Loss curve [14].

The calculation of the coincidence frequency takes place by using [16]

$$f_c = \frac{1}{2\pi} \sqrt{\frac{m}{B}} c^2 \frac{1}{\sin^2 \varphi} \quad [Hz] \quad (8)$$

where the variable B is the bending stiffness of the wall, m is the specific structural mass, and c is the sound velocity in the adjacent fluid. The angle φ describes the direction of the incident acoustical wave with respect to the normal of the structure.

3 Effect of different modelling variants of the stringers

The aim of the investigation in this section is to characterize the influence of different modeling variants of the stringers. First, the model variants are described in detail. Then the calculated structural behavior of the different variants as well as the acoustical effects are discussed. Finally, the reduction of the calculation costs is shown.

3.1 Description of the modelling variants

Four different finite element discretizations (modelling variants) of the stringer, which is displayed in Fig. 2, are investigated. These are

- Variant A:* Shell elements only
- Variant B:* Combination of shell and solid elements
- Variant C:* Combination of shell and beam elements
- Variant D:* Beam elements.

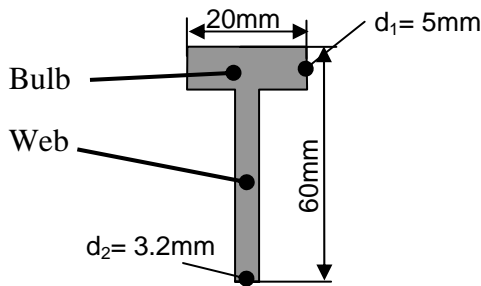


Fig. 2. Cross section of the investigated stringer.

The skin field of the structure is modelled using shell elements.

Shell modelling - variant A:

A view of the structural mesh of the variant A is shown in Fig. 3. The web, i.e. the vertical part of the stringer, is modelled with shell elements (thickness 3.2 mm) and the “bulb”, which denotes the top part of the stringer, is modelled by using shell elements (thickness 5 mm) as well.

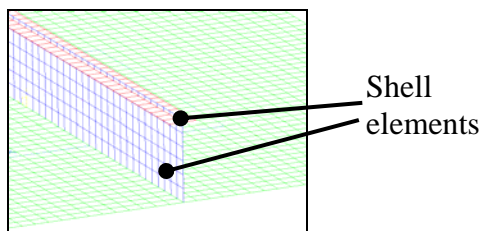


Fig. 3. Structural mesh variant A.

Shell and solid modelling - variant B:

The difference of this variant (see Fig. 4), in comparison to variant A, is the modeling principle of the bulb. This variant is chosen to investigate the behavior of shell elements with large thicknesses (5 mm). By increasing the thickness of the structure more and more, shear effects must be considered. However, this has been resolved here by using solid elements with more degrees of freedom as in the case of the shell variant.

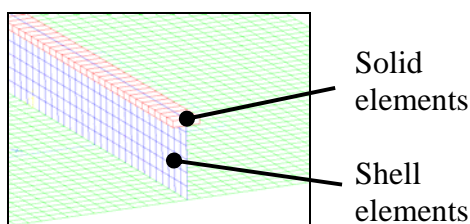


Fig. 4. Structural mesh variant B.

Shell and beam modelling-variant C:

In this variant the stringer bulb consist of beam elements (see Fig. 5). This type of elements may be used to model parts of the structure in a simplified way in order to reduce the degrees of freedom (dof), which is often an important concern especially for FE models of large structures. The cross section of the stringer bulb geometry is modelled as shown in Fig. 2.

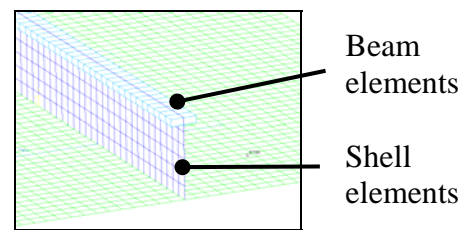


Fig. 5. Structural mesh variant C.

Beam modelling - variant D:

For this variant the complete stringer is modelled by beam elements only (see Fig. 6). In contrast to variant A where 500 nodes are necessary to model the stringer, in this case only 50 nodes are needed. Therefore this reduction of the degrees of freedom results in a significant decrease of the computational costs. However, the advantage of using beam elements must be considered with respect to a reduced accuracy of the computed results.

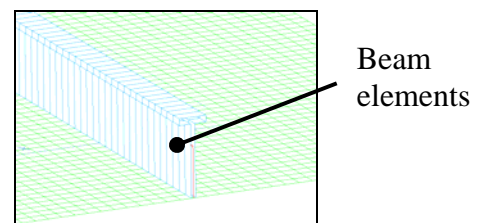


Fig. 6. Structural mesh variant D.

The discussion of the influences of the four different modelling variants is given in the following section.

3.4 Effects for the different modeling variants of the stringer

The structural behavior (mode shapes) of the different models introduced above shows partially deviant results. However, the first four

eigenmodes of all variants are nearly identical. In Fig. 7 an example for none existing mode shape of variant D is shown. Fig. 8 illustrates an example for the case where particular mode shapes are not found for variants A-C but they are observed for variant D. Such differences in the structural behavior of the variants lead to acoustical effects, because of additional modal deflections of the skin field. However, the expected influence occurs at discrete frequencies.

It has been found that in cases of typical skin modes the differences of the shapes and the eigenfrequencies of all four variants are negligible.

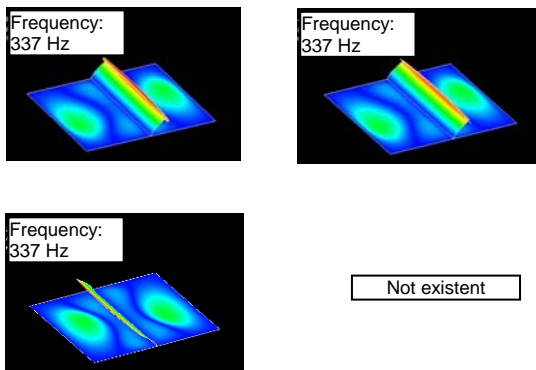


Fig. 7. Structural mode shapes of variants A-C. Mode shape of variant D does not exist.

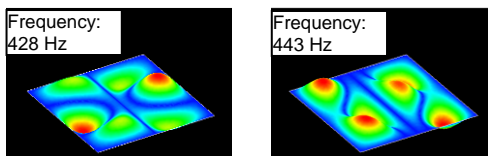


Fig. 8. Structural mode shapes for the variant D. Mode shapes of variants A-C do not exist.

The acoustical effects of the different stringer modeling variants and also the eigenfrequency shifts and missing mode shapes are explained by the TL diagram in Fig. 9. The variants B (shell solid) and D (beam) are displayed.

The deviation shown in region “a” can be explained by an eigenfrequency shift of the first mode. At this frequency the variant D is stiffer than the variant B.

The dip denoted at “b” results from the modes given in Fig. 7. As expected, no dip occurs in the curve of the beam variant, which

means no corresponding mode shape can be observed at this frequency.

The region “c” is dominated by a smaller number of strong mode shapes. The TL curve of variant D, for example, includes the two eigenfrequencies shown in Fig. 8. However, the only visible modal dip in the TL curve results from the skin field mode shown in Fig. 10. The respective region is marked by “d”. The two modes of Fig. 8 are less dominant and therefore no effects are visible in the TL curve. In the TL of variant B two dips are visible. The first dip occurs at a frequency of 420Hz and results from a combination of stringer and skin deflections (not observed in the case of the beam variant). The second dip is equivalent to the mode shape depicted in Fig. 10 and results from a typical skin field mode. The offset behind the peak at “d”, which can be observed up to 550Hz, can be explained by the significant influence of the mode shape at “d”.

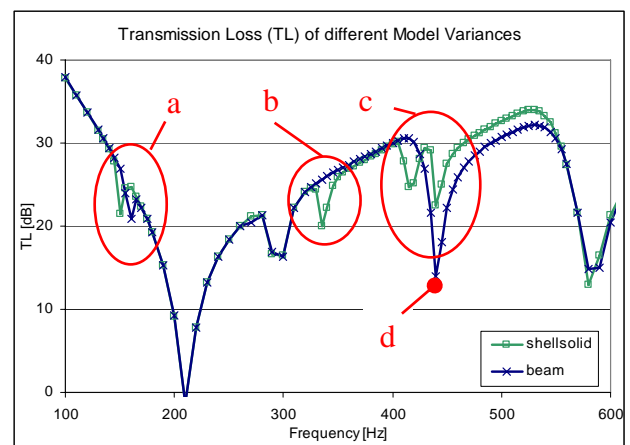


Fig. 9. Comparison of the Transmission Loss for the variants B and D.

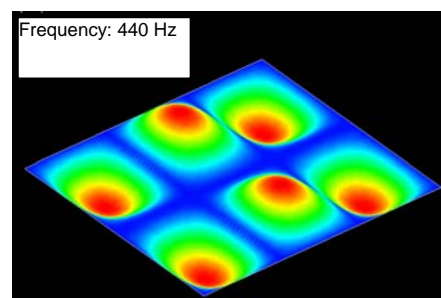


Fig. 10. Typical mode shape of a skin field for variant D at 440 Hz.

From the discussion above, the influence of different modelling variants becomes clear. The effects occur not only in a small frequency range but may also influence broad ranges of the solution. However, the calculation costs can be reduced drastically by accepting less accurate results, for instance, if beam elements are used. In the case of large structures like airplane fuselages, the application of beams can be sufficient.

It should be noted that from the acoustical point of view, the previous discussion has dealt with the effects caused by the skin fields only. The influence of the sound induced directly by the stringers has not been shown because of the size of the stringers and because of the rather low frequency range that has been considered. Hence, the investigation of this topic will be performed for larger stiffeners as described in section 4.3.

4 Acoustical effects of a large stringer

In this section the acoustical influence of stiffeners attached to the panel is investigated by including the stringer in to the acoustic BE model. The TL and the radiation efficiency will be calculated and two different effects will be discussed, namely the general acoustical impact of an oversized stringer and the effect of the sound radiation of the stringer itself.

4.1 Influence of the stiffening on plane plates

Using three different models, the effects of stiffening are shown considering the TL. The respective models are:

model 1: plane plate (no stringer attached),

model 2: plane plate with shell stringer,

model 3: plane plate with beam stringer.

4.1.1 Introduction of the models

Fig. 11 demonstrates the FE models used for the calculation of the structural behavior. The edge length of the plane plate is chosen to 0.5m and the thickness to 3.2 mm. The height of the stringer is 0,1m. The overall panel weight differs due to the mass of the stringer. The material parameter corresponds to typical values for aluminium. The boundary conditions of the models are chosen such that translational

movements are prevented and rotations are possible, commonly referred to as “simply supported” boundary conditions. For the BEM mesh the plane plate model in Fig. 11 (model 1) is employed.

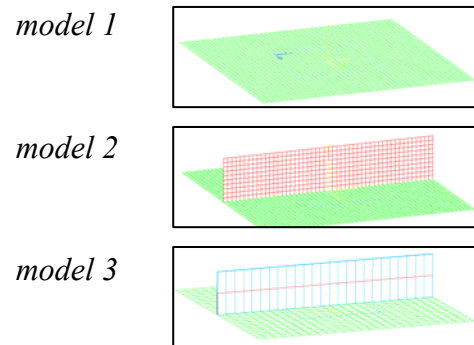


Fig. 11. Modelling variants for the investigation of acoustical influences.

4.1.2 Discussion of the calculated results

The calculated results for the three different models are shown in Fig. 12. The curve marked with “squares” represents the TL for the plane plate without stringer (model 1), the “cross marks” curve is equivalent to the beam stringer (model 2), and the “triangular marks” curve shows the TL for the stringer modeled by shell elements (model 3). The differences between the two stringer variants are obviously low (see section 3.4), while the differences compared to the plate without stiffeners is significant. In the lower frequency domain up to 800 Hz the influence of the eigenmodes is very obvious (see Fig. 1). In fact, the eigenfrequencies are shifted and therefore the modal differences caused by the stiffening of the plate lead to significant differences in the TL curves.

Besides these effects, a “local coincidence” resulting from certain parts of the skin field is existing at region “a”. The TL for model 1 shows a typical mass controlled frequency area, while the curves for the stiffened plates are influenced by the modal and by the coincidence effects. In region “b” and “c” coincidence effects for the perpendicular direction of wave propagation are shown. While for the “squared marks” curve only one coincidence region is observed (both coordinate directions have equal stiffness) the stiffened plates include two coin-

cidence frequencies each accounting for one direction of the wave propagation.

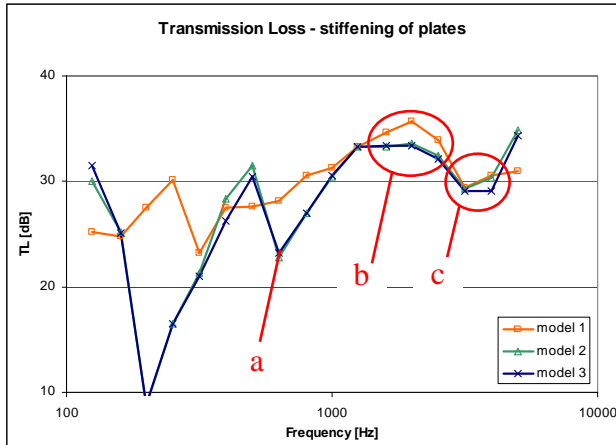


Fig. 12. Transmission loss through the plane plate without and with stiffeners.

4.2 Acoustic radiation of the stringers

In this section the sound radiation (radiation efficiency) of the stringers is discussed. Therefore two different calculations, based on the model 2 as described in section 4.1.1, are executed. While the structural input in both calculations is the same, the input models for the BEM analysis differ. In one case the stringer is included into the model, in the other case no stringer is modelled. The excitation of the structure is accomplished using a constant force over the frequency range.

The calculated results are shown in Fig. 13. In the frequency range around 1 kHz, the stringer model with the stringer is radiating more sound energy than the model without the stringer. The depicted mode shape of the stringer (1 kHz) shows slightly more than two wave lengths in the direction of the width of the stringer. The according wave length is 25 cm. The same wave lengths exist in the fluid at this frequency. Hence, the radiation of the stringer can be compared to a coincidence radiation. In general, the sound radiation is much more significant than in the case of the model without the stringer.

The next region emphasized in the Fig. 13 demonstrates the effect of the stringer deformation in the second direction. Here the radiation from the stringer seems to be negligible since no

differences between the models can be observed. In this case, no coincidence of the fluid and the structural wave lengths occurs.

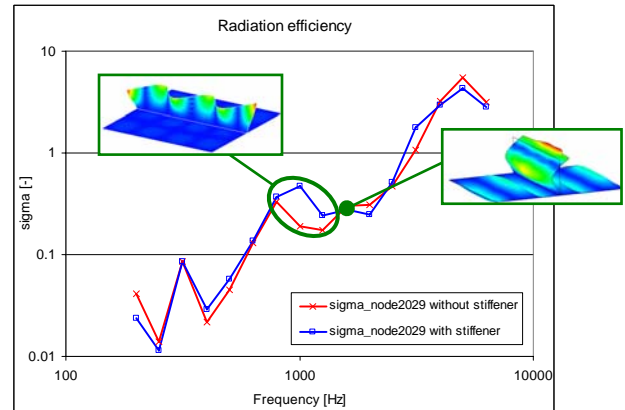


Fig. 13. Radiation efficiency of the plate without and with stiffeners.

5 Influence of different stiffening skins on the coincidence

In sections 3 and 4, the influences of plate stiffeners on the acoustics are presented. Especially the modal effects and the coincidence influence are discussed by regarding idealized geometries. In this section, a typical stringer construction is investigated to show the effects of realistic stiffeners. The edges of the models have been doubled in length and 6 stringers and 12 stringers are used, respectively. These more complex models give an idea of the interaction between the explained effects and the drastically influence on the acoustical behaviour.

5.1 Introduction of the model

Five different models have been investigated which are summarized in the following table:

BEM model	Plate	No stringer
variant I	plate+feet	6 stringer
variant II	plate+stringer	6 stringer
variant III	plate+feet+stringer	6 stringer
variant IV	plate+feet+stringer	12 stringer

As before, the BEM model is used for the acoustical calculations, while the variants I-IV define the different geometries of the structure.

The stringer size is equal to standard dimensions for an aircraft fuselage (see Fig. 14). The stringer feet are included by modifying the skin elements appropriately. Therefore the thickness of the concerned skin elements is bloated.

Thicknesses:

skin = 3.2mm
stringer = 2mm

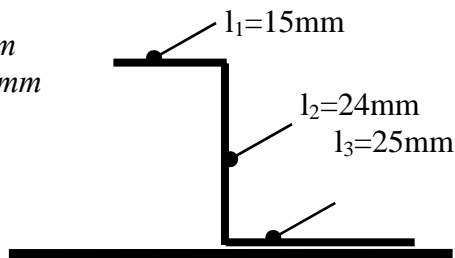


Fig. 14. Geometry of the realistic stringer

5.2 Discussion of the calculated results

Fig. 15 demonstrates the calculated TL for the four different models as introduced above.

A typical curve for a plane skin is given in the case of variant I. In the mass controlled region the curve increases constantly. At the skin field coincidence, however, the curve shows a significant dip, and for higher frequencies the slope of the curve becomes steeper.

Rather different characteristics are observed, if the feet used in variant I are replaced by stringers according to variant II. The coincidence dips span over a larger frequency range (see region “a”) and the mass law is not sufficient anymore to characterize the lower frequency range. A second coincidence drop occurs approximately between 1 kHz and 1.5 kHz. This effect can be explained by the stiffening of the plate in the direction aligned with the stringer.

The curve from variant III, where stringer and stringer feet are considered, shows a rather similar characteristic. The coincidence effect described above is more distinct (see region “b”).

Across the entire frequency range variant IV shows the lowest TL of all investigated variants. Compared to variant III, the strong stiffening of variant IV (6 stringers x-direction and 6 stringers y-direction) leads to a lower coincidence frequency, as indicated by region “c”.

This effect causes a decrease of the TL over a large frequency range. Above the skin field coincidence at 3.1 kHz (see region “a”) the characteristic of the TL curve is similar to all other variants.

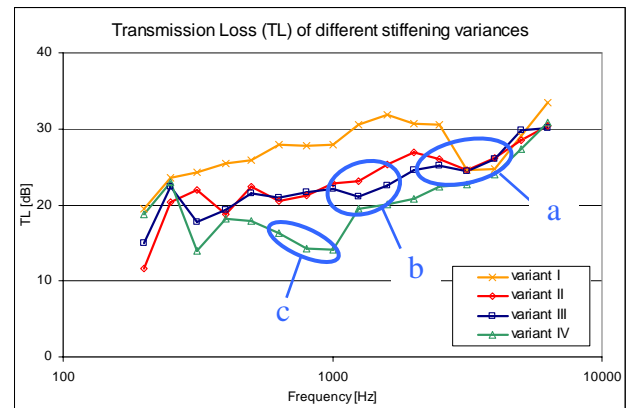


Fig. 15. Transmission Loss of panels with realistic stringers.

6 Conclusion

The objective of this paper was to illustrate the structural and acoustical effects in the case of stiffened panels. The applied computational approach is based on the coupling of the structural FEM, employed for the panel, with the indirect BEM, which is used to represent the acoustic domain.

A detailed analysis addressed the optimal choice of a discretization to be used when a stiffened structure shall be investigated numerically. It was found that an application of shell and solid elements leads to accurate results, while the application of only beam elements yields less accurate results. In the latter case, however, a significant reduction of the computation costs may be accomplished.

Moreover, the acoustical effects of different modelling variants have been shown and the effect of the acoustical radiation of the stringers themselves is demonstrated. Significant effects have been shown if coincidence effects occur.

A systematic investigation for a realistic panel stringer combination, where the different stiffening elements, such as stringer feed and web for each direction, were included in the numerical model successively, shows the effects on the TL results. The main influence can be

observed at the additional coincidence frequencies which can increase the transmission path drastically.

References

- [1] Vaicaitis R., Slazak M., *Noise Transmission Through stiffened Panels*. Columbia University New York 1980.
- [2] Onsay T., *Vibro-acoustic Behavior of Bread-Stiffened Flat Panels: FEA, SEA and Experimental Analysis*. Society of Automotive Engineers, Inc., Daimler-Chrysler Corporation 1998.
- [3] Van der Wal, H. *Technical Report: Numerical results on small scale test structures*. EU-Project: Friendly Aircraft Cabin Environment FACE, 2003.
- [4] Koval L. R., *Effect of air flow, panel curvature, and internal pressurization on field incidence transmission loss*. JASA vol. 59(6), pp. 1379-1385, 1976.
- [5] Bilong L., Fenh L., Nilson A., *Influence of overpressure on sound transmission through curved panels*. KTH Royal Institute of Technology, 2004.
- [6] Bilong L., Fenh L., Nilson A., *Sound transmission through curved aircraft panels with stringer and ring frame attachments*. KTH Royal Institute of Technology, 2004.
- [7] Szechenyi E., *Sound transmission through cylinder walls using statistical consideration*, JSV, vol 19, pp. 83-94, 1971.
- [8] Kassegne S.K., Reddy J.N., *Local Behavior of Discretely Stiffened Composite Plates and Cylindrical Shells*. Department of Mechanical Engineering, Texas A&M University.
- [9] Bathe K.J., *Finite Elemente Methoden*. Springer Verlag, 1990.
- [10] Petyt, M., *Introduction to finite element vibration analysis*. Cambridge University Press, 1990.
- [11] von Estorff, O. *Boundary Elements in Acoustics: Advances and Application*. Southampton WIT Press, 2000.
- [12] LMS Numerical Integration Technologies, *SYS-NOISE User Manual*. Rev. 5.4 , 1999.
- [13] Van der Wal, H. *Technical Report: Selected modeling Tools*. EU-Project: Friendly Aircraft Cabin Environment FACE, 2004.
- [14] Beranek L. *Noise and Vibration Control*. John Wiley & Sons, inc., 1971.
- [15] Henn H, Sinambari G.R. and Fallen M. *Ingenieurakustik*. 3st edition, Publisher, 2001.
- [16] L. Cremer, M. Heckl, *Körperschall - Physikalische Grundlagen und Technische Anwendungen*, Berlin Springer Verlag, 1996.